Polo-like kinase is required for synaptonemal complex disassembly and phosphorylation in mouse spermatocytes

Philip W. Jordan[1], Jesse Karppinen[1,2] and Mary A. Handel[1],*

[1]The Jackson Laboratory, Bar Harbor, ME 04609, USA
[2]College of the Atlantic, Bar Harbor, ME 04609, USA
*Author for correspondence (maryann.handel@jax.org)

Summary

During meiosis, accurate coordination of the completion of homologous recombination and synaptonemal complex (SC) disassembly during the prophase to metaphase I (G2/MI) transition is essential to avoid aneuploid gametes and infertility. Previous studies have shown that kinase activity is required to promote meiotic prophase exit. The first step of the G2/MI transition is the disassembly of the central element components of the SC; however, the kinase(s) required to trigger this process remains unknown. Here we assess roles of polo-like kinases (PLKs) in mouse spermatocytes, both *in vivo* and during prophase exit induced *ex vivo* by the phosphatase inhibitor okadaic acid. All four PLKs are expressed during the first wave of spermatogenesis. Only PLK1 (not PLK2–4) localizes to the SC during the G2/MI transition. The SC central element proteins SYCP1, TEX12 and SYCE1 are phosphorylated during the G2/MI transition. However, treatment of pachytene spermatocytes with the PLK inhibitor BI 2536 prevented the okadaic-acid-induced meiotic prophase exit and inhibited phosphorylation of the central element proteins as well as their removal from the SC. Phosphorylation assays *in vitro* demonstrated that PLK1, but not PLK2–4, phosphorylates central element proteins SYCP1 and TEX12. These findings provide mechanistic details of the first stage of SC disassembly in mammalian spermatocytes, and reveal that PLK-mediated phosphorylation of central element proteins is required for meiotic prophase exit.

Key words: Meiosis, Synaptonemal complex, G2/MI transition, Polo-like kinase, Spermatocyte

Introduction

Meiosis, a defining event of gametogenesis, is a specialized cell division involving one round of chromosome replication followed by two rounds of chromosome segregation (meiosis I and II), resulting in the formation of up to four haploid gametes. During the reductional meiosis I division, homologous chromosomes segregate and the sister chromatids remain associated until their segregation in the equational division of meiosis II. Unique and characteristic chromosomal events define prophase I and the transition from meiotic prophase I to metaphase I (G2/MI) (reviewed by Handel and Schimenti, 2010). During prophase I, homologous chromosomes recognize, pair and synapse with one another and undergo crossover recombination, processes that are essential for successful chromosome segregation. In most organisms, including mammals, homologous chromosome synapsis and recombination is facilitated by a zipper-like tripartite protein complex known as the synaptonemal complex (SC). The SC is comprised of two lateral elements that form the core of each homolog and a series of transverse filaments known as the central element, which bridges the two lateral elements. Precursors of the SC develop during the leptotene sub-stage of prophase I, when the cohesin complex, including meiosis-specific subunits REC8 (recombination 8) and STAG3 (stromal antigen 3), HORMA (Hop1–Rev7–Mad2)-domain containing proteins (HORMAD1 and 2) and the synaptonemal complex proteins SYCP2 and SYCP3 form the axial elements between sister chromatids (Yanowitz, 2010). Concurrently, the meiosis-specific topoisomerase-like enzyme, SPO11 introduces

double-strand breaks (DSBs) during leptonema. During the zygotene stage, homologous chromosomes become associated with one another via the initiation of inter-homolog recombination and SC formation, whereby the axial elements become the lateral elements of the SC and the central element, comprised of SYCP1, synaptonemal complex elements SYCE1, SYCE2, SYCE3 and testis expressed protein TEX12, links the homologs together (Yanowitz, 2010). During SC formation, HORMAD1 and 2 disassemble from regions that have synapsed (Wojtasz et al., 2009). By the pachytene stage, homologous chromosomes are fully synapsed and a subset of inter-homolog recombination events results in crossovers, which also hold homologs together. At this stage during spermatogenesis, the largely non-homologous X-Y chromosomes are synapsed at the pseudo-autosomal region (PAR) and transcriptionally silenced via chromatin modifications that form the X-Y body (Handel, 2004; Turner, 2007).

The crucial event of exit from meiotic prophase and initiation of the meiosis I division phase is desynapsis, or disassembly of the tripartite SC. The disassembly of the SC initiates during the diplotene stage, when components of the central element dissociate from the chromatin, remaining only at chromosome ends and sites of crossovers. HORMAD proteins relocalize to desynapsed regions at this stage (Wojtasz et al., 2009). During diakinesis, extensive chromosome remodeling and condensation occurs, the central element components completely dissociate, and the lateral element proteins also dissociate, but remain at the centromeres. Following diakinesis, further chromatin condensation leads to pairs of separate

(individualized) metaphase I homologs, with pairing now maintained by crossovers (visually manifest as chiasmata). These chiasmata are essential to ensure accurate chromosome segregation during anaphase of meiosis I; indeed the penalty of absence of crossovers is aberrant segregation and subsequent aneuploidy of gametes and offspring (Handel and Schimenti, 2010). Thus it is essential that desynapsis be precisely executed, timed and coordinated with completion of the molecular events of recombination. Studies with budding yeast have shown that failure to disassemble the SC results in aberrant chromosome segregation during meiosis I (Jordan et al., 2009). However, in mammalian spermatogenesis, the consequences are more severe; failure to form recombination crossovers (Edelmann et al., 1996; Lipkin et al., 2002) or failure to desynapse (Dix et al., 1997; Sun et al., 2010) both arrest meiosis at the G2/MI transition, thus abrogating the possibility of mal-segregation and ensuing sperm aneuploidy or infertility.

Previous studies have implicated several key features of the regulation of desynapsis and the G2/MI transition in mouse spermatocytes. First, it is under strict translational control (Sun et al., 2010); second, the chaperone protein HSPA2 is involved in critical events at the SC promoting desynapsis (Dix et al., 1997; Zhu et al., 1997); and, third, kinase activation controls many key processes of the G2/MI transition. Specifically, cyclin-dependent kinases (CDKs) and aurora kinases (AURKs) are required for disassembly of the lateral elements during the diplotene and diakinesis stages (Cobb et al., 1999; Sun and Handel, 2008). However, inhibitor analyses have suggested that neither CDKs nor AURKs are required for the first key step of desynapsis, namely, disassembly of the SC central element. Here we provide new evidence implicating polo-like kinase (PLK) in this process. The polo-like kinase (Cdc5p) in yeast is required for the disassembly of the SC central element during exit from meiotic prophase (Jordan et al., 2009; Sourirajan and Lichten, 2008). In mammals, there are five paralogs of polo-like kinases, PLK1–5, although key kinase residues are absent in PLK5 (de Cárcer et al., 2011). PLK1 is the mammalian ortholog of Cdc5p and is termed a 'master regulator' of cell division (de Cárcer et al., 2011). To probe the role of PLK in desynapsis, we have taken advantage of the nearly synchronous first wave of spermatogenesis in mice (Bellvé et al., 1977; Cohen et al., 2006) and the ability to isolate highly enriched pachytene spermatocytes and induce meiotic prophase exit *ex vivo* with the phosphatase inhibitor okadaic acid (OA) (Handel et al., 1995). We report that the four kinase-proficient PLKs are expressed during mouse spermatogenesis and that PLK1 is localized to the SC during the G2/MI transition. BI 2536, a small molecule inhibitor of PLK1 (Steegmaier et al., 2007), inhibits disassembly of the SC central element during the G2/MI transition. Moreover, we document phosphorylation dynamics of SC central element proteins during the G2/MI transition and the involvement of PLK1 in phosphorylation of these proteins. Taken together our findings provide robust evidence that PLK1 is required for the first step of desynapsis, the disassembly of the SC central element.
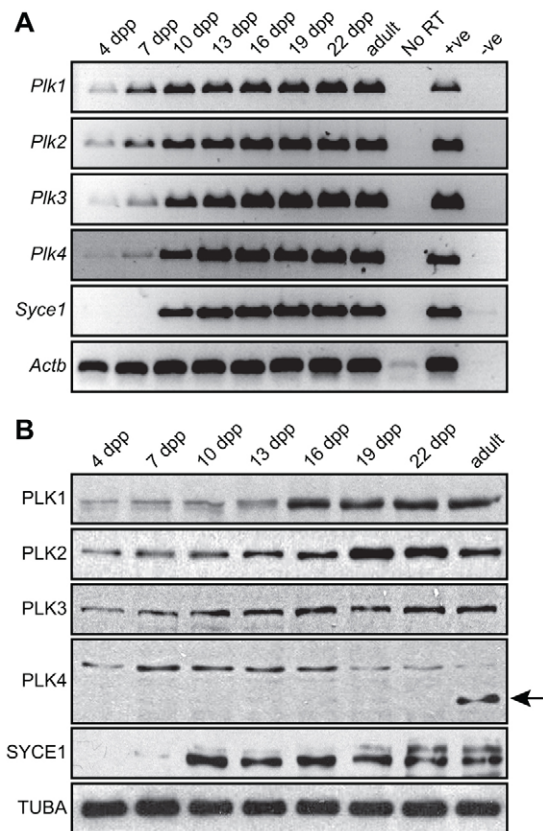
Results
Polo-like kinase gene and protein expression during the first wave of spermatogenesis
The pattern of expression of mRNA and protein of four polo-like kinases (PLK1–4) during different stages of spermatogenesis was analyzed in germ cells enriched from testes during the nearly synchronous first wave of spermatogenesis (Fig. 1). Transcripts

for *Plk1–4* increase with progression of the first wave of spermatogenesis (Fig. 1A), with expression at low levels at 4 days postpartum (dpp) when spermatogonia are present and then increasing to higher levels, particularly evident with onset of expression of the gene encoding a central element component of the SC, *Syce1*. To more clearly discriminate levels after onset of expression, a reduced cycle RT-PCR was assessed (supplementary material Fig. S1). Transcript levels from all four *Plk* genes were highest when late prophase spermatocytes were abundant (16 dpp) and when the leading edge of spermatogenic cells undergoes the G2/MI transition (19–22 dpp).

PLK1–4 proteins were detected throughout the first wave of spermatogenesis (Fig. 1B). Relative levels of PLK1, PLK2 and PLK3 protein are low when only spermatogonia are present, and higher when the G2/MI stage spermatocytes are abundant during the first wave of spermatogenesis (19–22 dpp), a pattern similar to that of a central element protein of the SC, SYCE1 (Fig. 1B). Relative levels of PLK4 are highest during the early and mid stages


Fig. 1. Expression of PLKs during the first wave of spermatogenesis. This figure provides representative results of analyses of RNA and protein extracted from germ cells of B6SJL F1 male mice aged 4, 7, 10, 13, 16, 19, 22 and 56 (adult) dpp. (**A**) PCR analysis of mRNA expression of *Plk1-4*; *Syce1* was used as a control for progression of the first wave of spermatogenesis and *Actb* was used as a mRNA loading control. mRNA extracted from whole testis and RNA-free H_2O were used as positive (+ve) and negative (−ve) controls, respectively (35 PCR cycles were used, see Materials and Methods). Each transcript was assayed at least four times. (**B**) Western blot analysis of PLK1–4 proteins; SYCE1 was used as a control for progression of the first wave of spermatogenesis and TUBA (tubulin) was used as a protein loading control. The faster migrating form of PLK4 detected in adult germ cells is indicated by a black arrow. Each protein was assayed at least two times.

of the first wave of spermatogenesis (7–16 dpp), then drop during the G2/MI transition stages (19–22 dpp). Mixed germ cells from adult testes have low PLK4 protein levels compared to germ cells from the first wave of spermatogenesis, perhaps reflecting the lower representation of meiotic cells. However, a prominent faster migrating protein band was detected by the PLK4 antibody in enriched germ cells from the adult testis; this protein may be a truncated or a splice variant form of PLK4, but has not yet been annotated by ENSEMBL or other annotation databases.

Localization of PLKs during meiosis

The localization of PLK1–4 during meiosis I was determined by immunofluorescence assessment of spermatocyte nuclear spreads (Fig. 2). During the leptotene and zygotene stages of meiotic
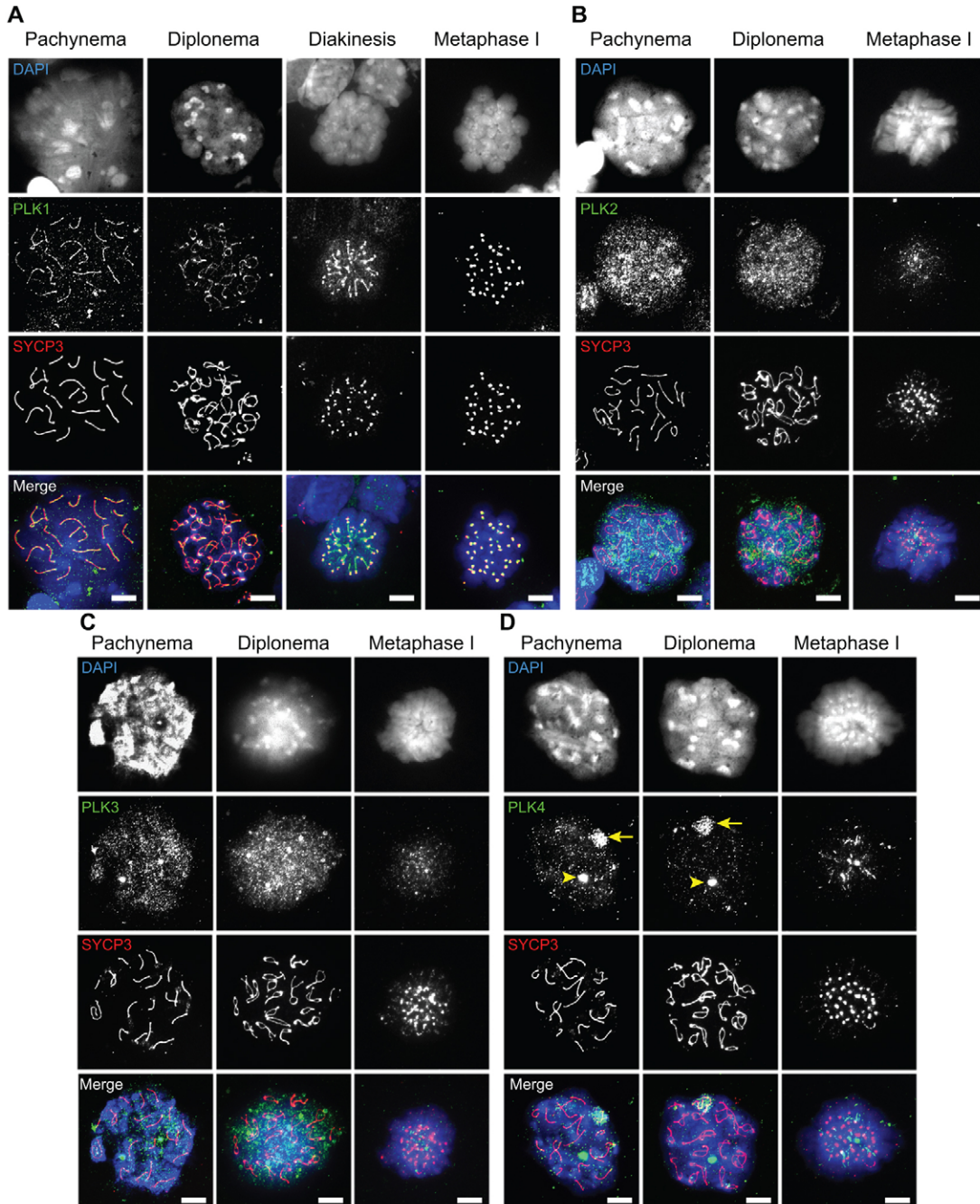
Fig. 2. Localization of PLK1–4 in male germ cells. Nuclear spreads from testicular germ cells of B6SJL F1 mice aged 19–23 dpp were stained with DAPI (blue) and immunolabeled using antibodies against PLKs (green) and the SC lateral element protein SYCP3 (red). (**A**) PLK1, (**B**) PLK2, (**C**) PLK3 and (**D**) PLK4. In D, the yellow arrowheads point to aggregates of PLK4 and the yellow arrows point to PLK4 that is localized to the X-Y body during pachynema and diplonema. At least 100 nuclear spreads at pachynema, diplonema and metaphase I were scored for each antibody, and three independent rounds of nuclear spread preparations were used for immunolabeling. Scale bars: 10 μm.

prophase I, PLK1 signal was observed in the chromatin (data not shown). By pachynema, PLK1 was seen in the SC, as shown by colocalization with signal from antibody against the lateral element protein SYCP3 (Fig. 2A). PLK1 continues to colocalize with the SC lateral element signals during diplonema, when the central element of the SC has disassembled. At diakinesis, when the lateral element disassembles and SYCP3 localizes to centromeres, PLK1 signal was observed as linear profiles between SYCP3 foci. By metaphase I, PLK1 was seen at the centromeres, colocalizing with SYCP3 signal.

In contrast to the SC localization of PLK1, PLK2 and PLK3 protein signals were observed in the chromatin throughout pachynema and diplonema (Fig. 2B,C). PLK4 signal was observed in the XY body at pachynema and diplonema, as well as in chromatin-associated aggregates (Fig. 3D). Localization of PLK4 to the XY body was confirmed by colocalization of signals for PLK4 and γH2AX (the phosphorylated form of histone H2AX, also known as H2AFX), which is known to accumulate in the XY body during pachynema and diplonema (supplementary material Fig. S2) (Fernandez-Capetillo et al., 2003). At metaphase I, PLK2, PLK3 and PLK4 signals were enriched at chromatin regions near the centromeres (Fig. 2B–D).

As a control, the antibodies used to determine the localization (and protein expression) of PLKs during meiosis were pre-incubated with the corresponding PLK proteins. All four pre-absorbed PLK antibodies, when used for immunofluorescence assessment of spermatocyte nuclear spreads, failed to recapitulate the localization patterns observed above (supplementary material Fig. S3), demonstrating their specificity.

SC disassembly kinetics induced *ex vivo*
Before analyzing PLK function, we refined and added to previously published landmarks of exit from meiotic prophase induced *ex vivo* (Cobb et al., 1999; Cobb et al., 1997; Sun and Handel, 2008). Pachytene spermatocytes from adult mice were enriched by sedimentation at unit gravity and subjected to short-term culture and treatment with the phosphatase inhibitor, okadaic acid (OA) as previously described (Handel et al., 1995). OA treatment initiates the G2/MI transition with exit from meiotic prophase, although a metaphase spindle is not formed in these conditions (Handel et al., 1995). The dynamics of SC central element and lateral element disassembly together with serine 10 phosphorylation of histone H3 were observed from immunolabeled nuclear spread preparations as previously reported (Cobb et al., 1999; Sun and Handel, 2008) (Fig. 3). Prior to the addition of 5 μM OA, 90% of cells exhibited fully synapsed autosomes and sex chromosomes synapsed at the pseudo-autosomal region (PAR; Fig. 3A–C). Approximately 2.5 hours after the addition of OA, most cells progressed to diplonema when the central element components of the SC were disassembled from the autosomes, remaining only at crossover recombination sites and chromosome ends (Fig. 3A–C). Additionally, phosphorylation of histone H3 Ser10 occurred at the heterochromatin-rich chromocenters (Fig. 3D,E). Interestingly, during this stage of prophase exit, SYCP1 labeling on the X-Y chromosomes is more extensive than immediate PAR localization (Fig. 3A), an observation reported previously for rat spermatocytes (Tarsounas et al., 1999), and one we have confirmed in freshly retrieved testicular spermatocytes (supplementary material Fig. S4). After 4 hours of OA treatment, most spermatocytes were observed to have progressed to diakinesis, when the lateral elements had disassembled from the autosomes and lateral

element component, SYCP3, remained at the chromosome ends (Fig. 3A–C) and histone H3 phosphorylation was evident throughout the chromatin (Fig. 3D,E). SYCP1 signal was still detected on the X and Y chromosomes at this stage, but levels were reduced (Fig. 3A). After 5 hours of OA treatment, most cells were observed to have reached metaphase I and SYCP1 signal was no longer present on the X and Y. As previously observed (Dobson et al., 1994; Sun and Handel, 2008), at MI, chromosomes were fully condensed and SYCP3 was localized at the centromeric ends of the chromosomes (Fig. 3A–C).

## BI 2536 inhibition of disassembly of central and lateral elements of the SC
Having established these landmarks, we assessed the effect of the PLK inhibitor BI 2536 on G2/MI progress. First we tested its effect on phosphorylation of the centromeric protein MLF1IP (myeloid leukaemia factor 1 interacting protein). During the mitotic G2/M transition MLF1IP is phosphorylated by PLK1 (Kang et al., 2006). During OA-induced prophase exit, MLF1IP was also phosphorylated (Fig. 3F). When 100 nM of BI 2536 was added to cultured pachytene spermatocytes, OA-induced MLF1IP phosphorylation was inhibited (Fig. 3G), providing evidence that BI 2536 inhibits this activity of PLK1 in spermatocytes.

When pachytene spermatocytes were treated with 100 nM BI 2536 and OA, the OA-induced disassembly of the SC central and lateral elements was inhibited (Fig. 3B,C; supplementary material Fig. S5A–F). Interestingly, although SC disassembly was inhibited by BI 2536, SYCP1 localization along the XY chromosome pair was still observed (supplementary material Fig. S5B). The effect of BI 2536 on OA-induced disassembly of the meiotic cohesin subunit, REC8 from the chromosomal axes was also assessed (supplementary material Fig. S5). When cultured pachytene spermatocytes were treated with OA, REC8 was disassembled with kinetics similar to the SC lateral element component, SYCP3 and by 5 hours axial REC8 was absent in more than 90% of cells (supplementary material Fig. S5G). In the presence of BI 2536, REC8 was retained, as were components of the SC (supplementary material Fig. S5B,G). These results provide evidence that PLKs are required for SC disassembly in spermatocytes, as in yeast (Sourirajan and Lichten, 2008).

As previously observed and attributed to AURK activity (Sun and Handel, 2008), OA-induced phosphorylation of the serine 10 residue of histone H3 was observed (Fig. 3D,E). However, in the presence of BI 2536, only 27% of cultured pachytene cells showed evidence of H3 phosphorylation, compared to 100% of cells treated with OA only (Fig. 3E), and, moreover, although not quantified, the intensity of fluorescent signal per nucleus for H3 phosphorylation was lower in those BI 2536-treated spermatocytes that did show H3 phosphorylation. This reduction in H3 phosphorylation dynamics suggests that PLK function could be upstream to H3 phosphorylation. This is consistent with the fact that disassembly of the central element occurs prior to H3 phosphorylation (Sun and Handel, 2008). Alternatively, BI 2536 may directly and/or indirectly inhibit phosphorylation of non-PLK substrates (Santamaria et al., 2010).

BI 2536 inhibition of modification and degradation of components of the SC
Western blotting analyses of pachytene spermatocytes treated with OA in the presence or absence of BI 2536 were used to
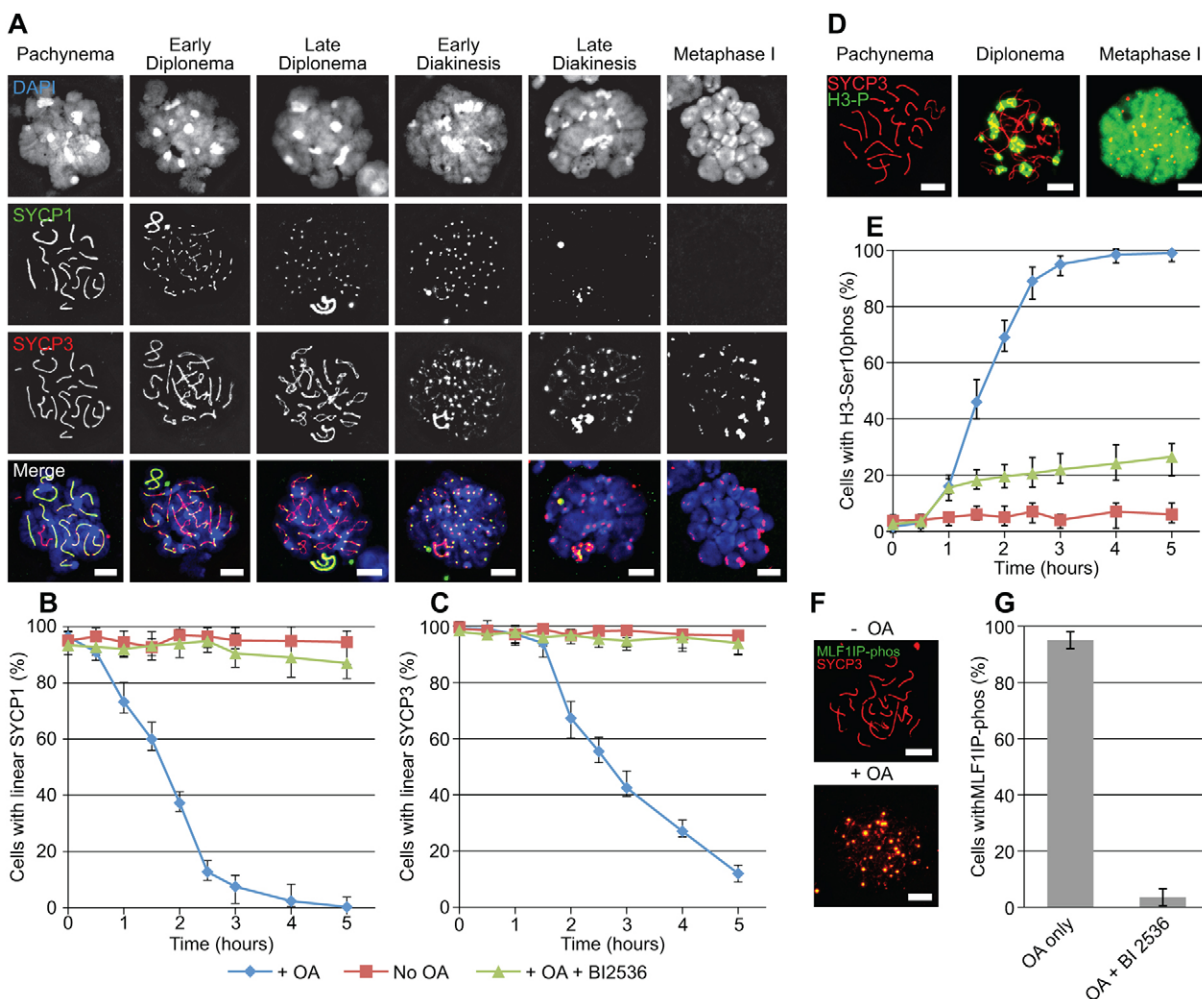
Fig. 3. SC disassembly during the OA-initiated G2/MI transition is inhibited by PLK inhibitor BI 2536. (**A**) Nuclear spreads from STAPUT-purified germ cells depicting steps in post-pachynema prophase exit induced by OA. Nuclear spreads were stained with DAPI (blue) and immunolabeled using antibodies against the SC central element component SYCP1 (green) and the SC lateral element component SYCP3 (red). (**B**) Time course of the disassembly of the SC central element component SYCP1 during OA-initiated G2/MI transition. STAPUT-purified pachytene spermatocytes were cultured without OA (red line, squares), with 5 µM OA (blue line, diamonds) or with 5 µM OA and 100 nM BI 2536 (green line, triangles). (**C**) Time course of the disassembly of the SC lateral element component SYCP3 during OA-initiated G2/MI transition. Graph details are as in B. (**D**) Nuclear spreads from STAPUT-enriched germ cells depicting phosphorylation of the serine 10 residue of histone H3 during the OA-initiated G2/MI transition. Nuclear spreads were immunolabeled using antibodies against phosphorylated H3 (green) and the SC lateral element component SYCP3 (red). Nuclear spreads staged at pachynema (pre-OA treatment), and post-OA diplonema and metaphase I stages are presented. (**E**) Time course for phosphorylation of the serine 10 residue of histone H3 during OA-initiated G2/MI transition. Graph details are as in B. (**F**) Nuclear spreads from STAPUT-enriched germ cells depicting phosphorylation of the threonine 78 residue of centromeric protein MLF1IP during OA-initiated G2/MI transition. Nuclear spreads were immunolabeled using antibodies against phosphorylated MLF1IP (green) and the SC lateral element component SYCP3 (red). (**G**) Bar graph presenting the number of nuclear spreads with phosphorylated MLF1IP after 5 hours in culture with 5 µM OA or with 5 µM OA and 100 nM BI 2536. For all experiments, at least 200 nuclei were counted per time point; experiments were performed in triplicate. Scale bars: 10 µm.

extend cytological observations and provide evidence for modifications of SC and cohesin proteins during the G2/MI transition (Fig. 4). OA-induced prophase exit was assessed by Ser10 H3 phosphorylation; consistent with immunocytology results (Fig. 3D,E), BI 2536 reduced the H3Ser10 phosphorylation levels (Fig. 4A). Modification of central element protein SYCP1 was apparent in OA-treated spermatocytes from retardation of its migration on an SDS PAGE gel (Fig. 4B). Additionally, modification of other central element proteins, TEX12 and SYCE1, in OA-treated spermatocytes was apparent from the appearance of slower migrating bands on an SDS PAGE gel (Fig. 4B). Treatment with

BI 2536 inhibited modification of TEX12 and SYCE1 and partially inhibited modification of SYCP1 (Fig. 4B). The SC central element protein SYCE3 was partially degraded after OA treatment, and this was inhibited by BI 2536 (Fig. 4B). Lateral element protein SYCP2 was also modified after OA treatment and this effect was inhibited by BI 2536 (Fig. 4C). Meiotic-specific cohesin subunits STAG3 and REC8 were degraded after OA treatment; these events were inhibited by BI 2536 (Fig. 4D). Furthermore, intensity of the slower migrating band of REC8 was reduced in the presence of BI 2536, regardless of addition of OA. Finally the HORMA-domain-containing proteins (HORMAD1 and 2) that localize to desynapsed axes at diplotene (Wojtasz
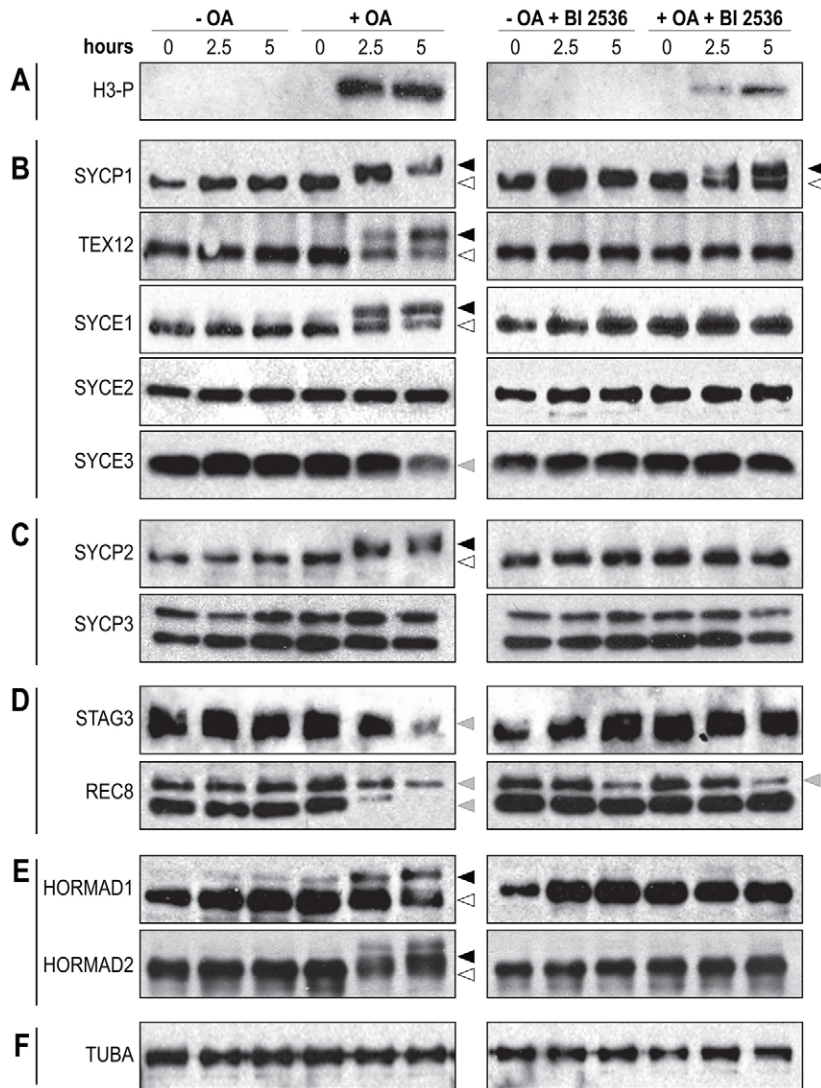
Fig. 4. Modification of SC components during OA-initiated G2/MI transition is inhibited by BI 2536. STAPUT-isolated pachytene spermatocytes were cultured without OA, with 5 µM OA, with 100 nM BI 2536 or with 5 µM OA and 100 nM BI 2536. Protein extracts were made at 0, 2.5 and 5 hours after initiation of treatment and western blot analyses performed for (**A**) serine 10 histone H3 phosphorylation; (**B**) SC central element proteins SYCP1, TEX12, SYCE1, SYCE2 and SYCE3; (**C**) SC lateral element proteins SYCP2 and SYCP3; (**D**) meiotic cohesin components REC8 and STAG3; and (**E**) HORMA-domain-containing proteins HORMAD1 and HORMAD2. (**F**) Tubulin (TUBA) was used as a loading control. White arrowheads point to the faster migrating protein signals; black arrowheads point to the slower migrating protein signals; grey arrowheads point to reduced protein signals (protein degradation). The results presented are typical from experiments repeated at least two times.

et al., 2009) also showed modification during prophase exit; these modifications were inhibited by BI 2536 (Fig. 4E). Because BI 2536 is a PLK kinase inhibitor, we hypothesize that the protein modifications observed during the G2/MI transition are phosphorylation events stimulated by PLKs.

### Phosphorylation of SC central and lateral elements during SC disassembly

OA, a phosphatase inhibitor, acts in part by preventing activation of kinases that regulate cell cycle progression. We hypothesized that phosphorylation accounts for mobility shifts of SC central and lateral element proteins after OA treatment of pachytene spermatocytes. Protein extracts from OA-treated spermatocytes were used in phosphatase assays to test this hypothesis. Dephosphorylation of the serine 10 residue of histone H3 was used as a control to determine both that calf-intestine phosphatase (CIP) activity was evident and that its activity was successfully inhibited by the commercial phosphatase inhibitor, PhosSTOP (Fig. 5A). From these phosphatase assays, it is clear that central element proteins TEX12, SYCE1 and SYCP1 (Fig. 5B), lateral element protein SYCP2 (Fig. 5C) and HORMAD1 and 2 (Fig. 5D) were phosphorylated during OA-induced SC

disassembly. Importantly, this modification also occurs *in vivo* and is apparent from analysis of SYCP1, TEX12 and SYCE1 from germ cells enriched from testes during the first wave of spermatogenesis (Fig. 5E), at a time (22 dpp) when G2/MI spermatocytes are represented at a high frequency. Indeed, dynamic changes in modification occur during the first wave of spermatogenesis. SYCE1 (Fig. 1B) appeared as a single band before diplotene spermatocytes are abundant (10–16 dpp), but a slower migrating band became evident when spermatocytes undergoing desynapsis were abundant (19–22 dpp). As revealed by the phosphorylation assay in Fig. 5E, the slower migrating SYCE1 band represents a phosphorylated variant. It is conceivable that SYCE1 is phosphorylated during desynapsis as it is removed from the SC. Together, these analyses provide evidence that phosphorylation of SC components occurs after OA treatment (Fig. 5) and are the modifications inhibited by the PLK inhibitor BI 2536 (Fig. 4) that are inferred to be required for SC disassembly (Fig. 3).

PLK1 phosphorylation of SYCP1 and TEX12 *in vitro*
To provide more direct evidence for the role of protein phosphorylation in disassembly of SC central elements
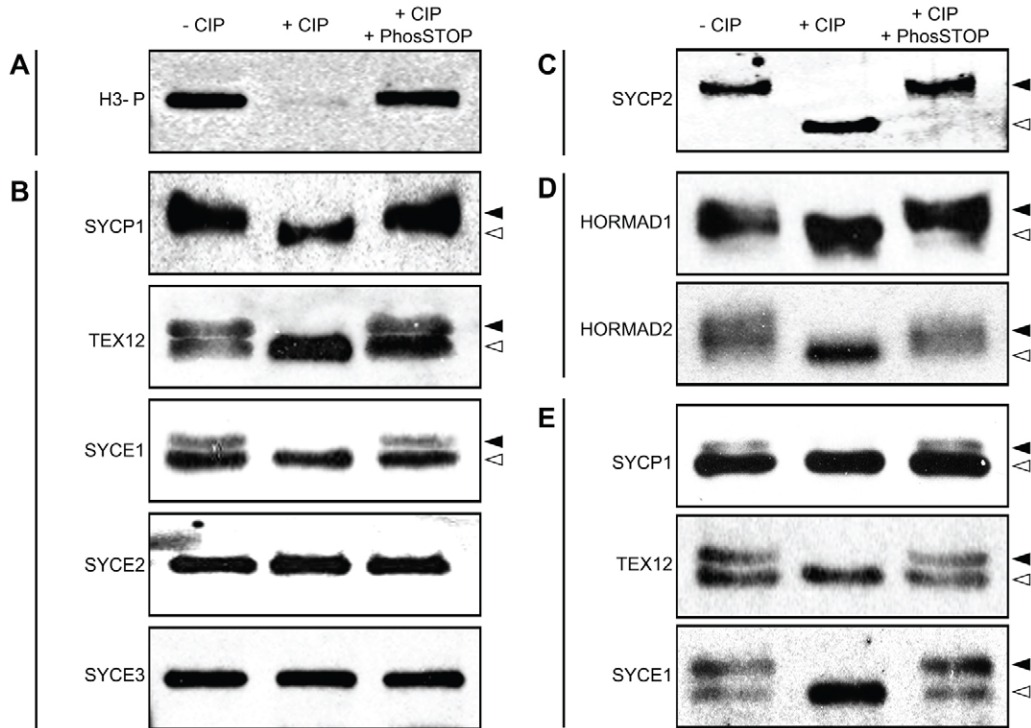
Fig. 5. SC components are phosphorylated during the G2/MI transition. STAPUT-enriched pachytene spermatocytes were cultured for 5 hours in 5 µM OA to induce the G2/MI transition, protein was extracted from the spermatocytes and used to assess protein phosphorylation of SC components in a standard calf intestinal phosphatase (CIP) assay. Protein extracts were analyzed in the absence of CIP (−CIP), in the presence of CIP (+CIP) and in the presence of CIP and the phosphatase inhibitor cocktail PhosSTOP (+CIP +PhosSTOP). Product of the CIP assays was used for western analysis of (**A**) serine 10 histone H3 phosphorylation; (**B**) central element proteins SYCP1, TEX12, SYCE1, SYCE2 and SYCE3; (**C**) SC lateral element protein SYCP2; and (**D**) HORMA-domain-containing proteins HORMAD1 and HORMAD2. (**E**) Analysis of protein extracted from enriched germ cells of male C57BL/6J mice (22 dpp) in a CIP assay to determine *in vivo* phosphorylation state of central element proteins SYCP1, TEX12 and SYCE1. White arrowheads point to the faster migrating dephosphorylated protein signals; black arrowheads point to the slower migrating phosphorylated protein signals. Each CIP assay was performed a total of three times.

inhibited by BI 2536, it was important to establish whether purified SC central element proteins can be directly modified by PLKs. Three central element proteins, SYCP1, TEX12 and SYCE1, are phosphorylated upon the OA-initiated G2/MI transition of pachytene spermatocytes (Fig. 4B; Fig. 5B). Therefore, we used an *in vitro* kinase assay to determine if PLK1, 2, 3 or 4 exhibit phosphorylation activity toward SYCP1, TEX12 and SYCE1 (Fig. 6, and data not shown). By this kinase assay, SYCP1 was shown to be phosphorylated by PLK1 (Fig. 6A,B); phosphorylation was inhibited by BI 2536 and not observed using the corresponding vector control. Additionally, PLK1-mediated SYCP1 phosphorylation was also observed using a second commercial source of purified PLK1 kinase (supplementary material Fig. S6A). The other PLK kinases (PLK2–4) failed to phosphorylate SYCP1 *in vitro*, resulting in background signal similar to that seen for the substrate only control (Fig. 6A; supplementary material Fig. S6A). Because modification of SYCP1 was not completely inhibited by BI 2536 (Fig. 4B), we considered the possibility of phosphorylation by other kinases. SYCP1 contains a polo-binding domain (PBD) binding motif (S-T/Sp-P) (Elia et al., 2003), a motif known to be phosphorylated by CDK1/CYCB1 (Park et al., 2010). Therefore we assessed phosphorylation of SYCP1 by CDK1/CYCB1, and found a band corresponding to the size of SYCP1 in the CDK1/CYCB1 kinase assay (Fig. 6A; supplementary material Fig. S6A), suggesting that SYCP1 can be phosphorylated by both

PLK1 and CDK1/CYCB1 kinases. However, other bands not corresponding to the size of SYCP1 were also evident. Furthermore, the SYCP1 phosphorylation signal intensity in the CDK1/CYCB1 kinase assay was more than eightfold less than that observed for the PLK1 kinase assay (Fig. 6A; supplementary material Fig. S6A). Control kinase assays with known PLK substrates were performed to confirm the enzymatic activity of the recombinant PLK2, PLK3 and PLK4 proteins used (supplementary material Fig. S7).

TEX12–GST was also phosphorylated *in vitro* by PLK1 but not by PLK2 (Fig. 6C,D). Although PLK3 and PLK4 exhibited kinase activity toward TEX12–GST, the signals were more than tenfold less than those observed for PLK1. Furthermore, other bands not corresponding to the size of TEX12–GST were evident at equivalent or higher signal intensity. BI 2536 inhibited PLK1-mediated phosphorylation of TEX12–GST. Additionally, the GST control substrate signal was similar to that of PLK1 without a substrate, suggesting that only background phosphorylation events were evident. The *in vitro* kinase analysis was repeated with a TEX12–6*His substrate, which confirmed that PLK1 phosphorylates TEX12, whereas PLK2–4 give signals that were at least 20-fold less than that observed for the PLK1 kinase assay (supplementary material Fig. S6B). We also assessed whether SYCE1–GST and SYCE1–6*His substrates were phosphorylated by PLK1; only very low phosphorylation signals were observed in these assays (data not shown).
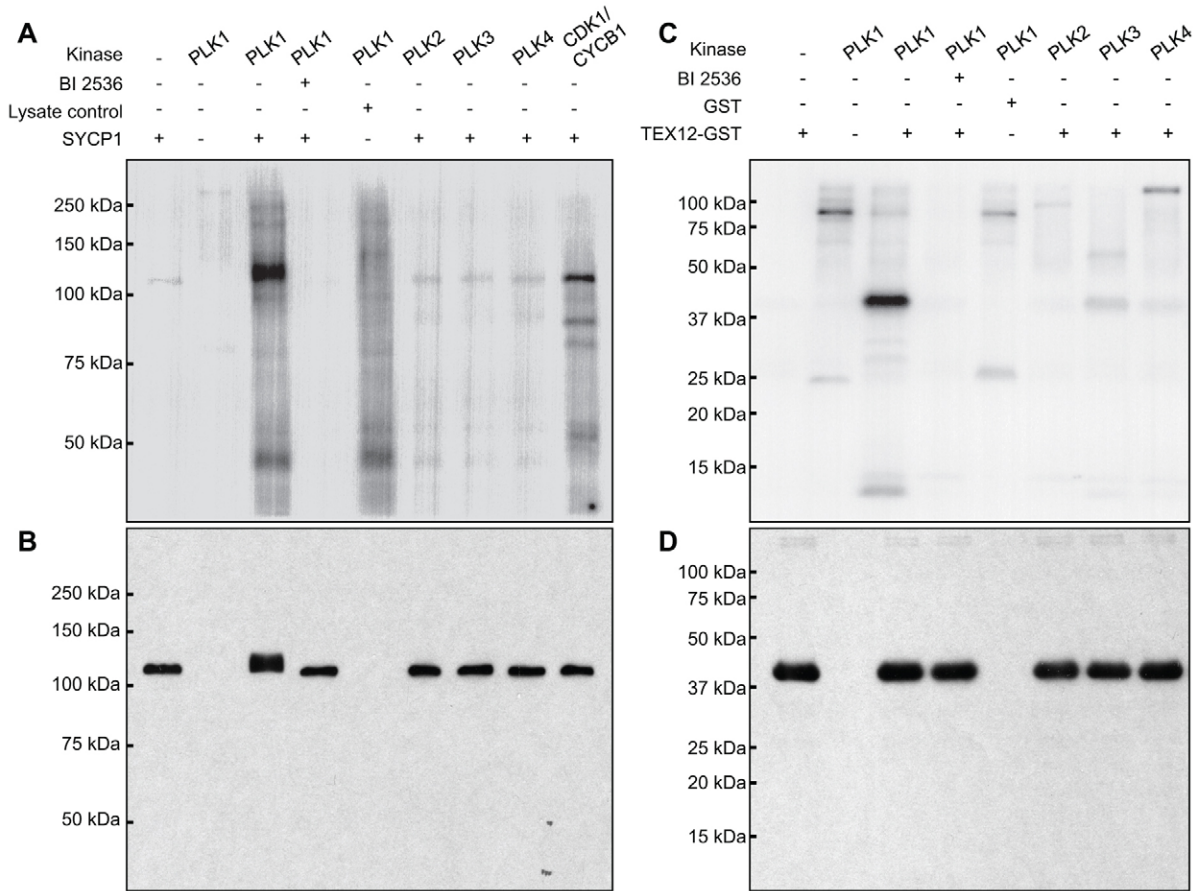
Fig. 6. *In vitro* phosphorylation of SC central element proteins by PLK1. (**A**) Purified SYCP1 protein or control cell lysates were used as substrates for kinase assays with PLK1, 2, 3, 4 or CDK1/CYCB1. The expected molecular mass of unmodified SYCP1 is 114 kDa. (**B**) Western blot analysis of SYCP1 protein used for the *in vitro* kinase assay. (**C**) Purified TEX12–GST protein or control GST protein were used as substrates in kinase assays with PLK1, 2, 3 or 4. The expected molecular mass of unmodified TEX12–GST is 40 kDa. (**D**) Western blot analysis of TEX12–GST protein used for the *in vitro* kinase assay. Signals in A and C reflect autoradiographic detection of $[\gamma\text{-}^{32}P]$ incorporation. The *in vitro* kinase assays were performed a total of three times.

Discussion

The data reported here reveal that PLK1 localizes to the SC before and during the G2/MI transition, that phosphorylation of central element proteins accompanies SC disassembly, that SC disassembly is inhibited by the PLK inhibitor BI 2536, and that purified PLK1 phosphorylates SC central element proteins *in vitro*. The experimental design, capitalizing on our ability to manipulate exit from meiotic prophase by mammalian spermatocytes *ex vivo*, allowed us to focus on PLK function at this critical stage, apart from any function that it might have earlier in meiotic prophase. Together these data provide robust evidence for PLK1 as a key player in the events that trigger spermatocytes to exit meiotic prophase. These findings prompt several key questions, the considerations of which provide deeper insight into this important meiotic event: How does PLK1 localize to the SC and is it a structural component of the SC? What signals prompt the local activation of PLK1 and other kinases mediating SC disassembly and de-synapsis? What is the role of phosphorylation in SC disassembly and removal of central element proteins?

PLK1, the SC and desynapsis

Proteins that function in desynapsis must be at least transiently localized in the SC, positioned to exert effect on central element proteins that maintain synapsis. Here we show that PLK1 is present at the SC in pachytene-stage spermatocytes, and that, by metaphase I, it relocates to the centromeres, colocalizing with several other SC proteins that also re-distribute to the centromeric ends of the chromosomes during the G2/MI transition. This is a similar localization pattern observed for a PLK1 ortholog in *Caenorhabditis elegans* (Harper et al., 2011; Labella et al., 2011). In contrast, the other three kinase-proficient PLKs, PLK2–4 do not localize to the SC, further implicating PLK1 specifically in desynapsis. Moreover homozygous deletions of *Plk2* or *Plk3* do not result in fertility defects in mice (Ma et al., 2003; Myer et al., 2011). Like *Plk1, Plk4* is essential for cell viability and its meiotic role has not been definitively tested, although when heterozygous, an ENU-induced Plk4 mutation within the kinase domain (*Plk4^{m1Lja}*) causes a testicular phenotype of focal regions of germ-cell loss (Harris et al., 2011), but not meiotic arrest or infertility. Our finding that PLK4 is sequestered to the X-Y body during pachynema and diplonema could implicate a role in meiotic sex chromosome inactivation (Royo et al., 2010).

Although our results imply an important role for SC-localized PLK1 in desynapsis, they do not exclude other meiotic roles within the context of the SC. Recently, it has been shown that two of three PLK1 subfamily genes (plk-1 and plk-2) in *C. elegans*

localize to the chromosome pairing centers during early prophase, with roles in early events of nuclear envelope remodeling and fidelity of the pairing process (Harper et al., 2011; Labella et al., 2011). Additionally, Cdc5p, the budding yeast polo-like kinase, regulates the completion of crossover recombination as well as SC disassembly (Clyne et al., 2003; Sourirajan and Lichten, 2008), again suggesting SC-localized function. Because the design of our study precluded discovery of early prophase roles for the PLKs, it is not known if they might play similar roles in pairing and recombination in mammalian meiocytes.

These lines of evidence suggest several important roles for PLKs in the structural context of the SC. Yet surprisingly little is known about how PLKs become structurally integrated into the SC, or how tightly they are associated. Interestingly, SYCP1 contains a polo-box domain (PBD) binding motif (S-T/Sp-P), and this motif could be important for localization of PLK1 to the SC. Polo kinases all contain one (PLK4) or two (PLK1–3) polo-box domains, which can play important roles in subcellular localization (reviewed by Park et al., 2010). Moreover, studies on PLK function in mitotically dividing somatic cells suggest that it is closely integrated with sub-nuclear structures. PLK1 associates with centrosomes during mitotic prophase, is enriched at kinetochores in prometaphase and metaphase, and is recruited to the central spindle at anaphase, foreshadowing its accumulation in the midbody at telophase (Petronczki et al., 2008). Additionally, PLK1 has been recently shown to localize to chromosome axes at the time of chromosome condensation during transition out of mitotic prophase (Abe et al., 2011). This is consistent with our demonstration of PLK1 localization to the SC and with its similar localization in *C. elegans* (Harper et al., 2011; Labella et al., 2011), suggesting the possibility that PLKs interact with chromosome axial components (e.g. cohesins and condensins), which may be a clue to its integration into the SC in a strategic position for bringing about desynapsis.

PLK1, desynapsis and meiotic prophase exit

Although some proteins important for the G2/MI transition of mammalian spermatocytes have been identified (Cobb et al., 1999; Cobb et al., 1997; Sun and Handel, 2008), the full repertoire of proteins required for the initiating event of desynapsis is not known. Here we focused on this event specifically, taking advantage of both the first wave of spermatogenesis and our ability to initiate and analyze in detail steps in the G2/MI transition in enriched mouse pachytene spermatocytes. The efficacy of the PP1 and PP2A protein phosphatase inhibitor OA (Handel et al., 1995; Wiltshire et al., 1995) in prompting the G2/MI transition suggests an antagonistic relationship between phosphatases and kinases, whereby phosphatases maintain the lengthy prophase and kinases initiate the G2/MI transition (Wiltshire et al., 1995). We sought evidence for PLK function by taking advantage of recent development of highly specific PLK inhibitors, an effort propelled by their potential use in cancer treatment (Strebhardt, 2010). BI 2536 was designed to inhibit PLK1, and indeed, when somatic cells are treated with BI 2536, they recapitulate the G2/M arrest observed when PLK1 is knocked down by RNAi (Steegmaier et al., 2007). BI 2536 has been shown to be at least 2000-fold more specific to PLK than to a large panel of other kinases (Steegmaier et al., 2007); however, it is only 4.5- and 11-fold more specific to PLK1 than PLK2 and PLK3, respectively. Given that the specificity of

BI 2536 is not absolute, the role of PLK1 in desynapsis and the spermatocyte G2/MI transition is best inferred from several independent lines of evidence.

The effect of BI 2536 on desynapsis was tested using the *ex vivo* OA-induced prophase exit assay. As shown, BI 2536 inhibited desynapsis and removal of the central elements from the SC, the initiating events of the G2/MI transition. Interestingly, these events are not prevented by CDK1 and AURK inhibitors (Sun and Handel, 2008), showing that they are not an effect of generalized kinase inhibition. Further evidence that it is PLK1 among the polo kinases that plays a key role in desynapsis is that only PLK1 (and not PLK2–4) that localizes to the SC during the G2/MI transition, and that two SC central proteins (SYCP1 and TEX12) are phosphorylated *in vitro* by PLK1 but not by PLK2–4. Thus, the weight of several independent lines of evidence suggests that the PLK1 is required for SC central element disassembly during the G2/MI transition in mammalian spermatocytes.

These findings are notable because they provide the first evidence implicating a specific protein in initiating exit from meiotic prophase in mammalian spermatocytes. Although a role for PLK1 in meiotic exit is evident from these findings, we do not know if it also acts earlier, how it is activated at meiotic prophase exit, what other proteins might be involved in coordinating these early events of the transition from meiotic prophase to metaphase, or, indeed, what initiates these events. It may be active 'initiation', or there may be 'release from inhibition' that propels spermatocytes out of meiotic prophase. For example, in *Drosophila*, *Xenopus* and mouse oocytes, inhibition of PLK1 maintains prophase arrest (Kishimoto, 2003; Shen et al., 2010; Xiang et al., 2007). Certainly both SC dynamics and repair of SPO11-induced DSBs involved in meiotic recombination must be coordinated for timely completion of meiotic prophase. The Cdc5p polo-like kinase of budding yeast apparently plays such a role, as it is the only factor required for both resolution of recombination events as crossovers and SC disassembly (Sourirajan and Lichten, 2008). Moreover, Mms4p (the ortholog in mammals is EME1) is phosphorylated by Cdc5p; this modification is required for activation of the Mus81–Mms4 complex to stimulate crossover recombination events (Matos et al., 2011). In mice, although the *Mus81* gene is not essential for fertility, it is required for repair of a subset of meiotic DSBs and regulation of crossover frequency (Holloway et al., 2008). Future studies of possible interactions among PLK1, EME1 and MUS81 in mammalian spermatocytes could lead to identification of signals that initiate the G2/MI transition. Additionally, the MLH1–3 complex is required for fertility and crossover recombination in mammals (Edelmann et al., 1996; Lipkin et al., 2002). This complex localizes to late crossover recombination nodules at pachytene (Moens et al., 2002), and these proteins are removed from the SC during the G2/MI transition. Moreover large-scale phospho-proteome analysis found evidence that the PBD sequence of MLH1 is phosphorylated within the testis (Huttlin et al., 2010). Together, these lines of evidence suggest that one possible signal for initiation and coordination of completion of recombination with desynapsis could be phosphorylation of MLH1; whether this is upstream to or downstream of PLK1 activation is an important question to resolve.

PLK1, SC protein phosphorylation and SC disassembly

Previous to this study it was clear that phosphorylation is required to stimulate the G2/MI transition, but the identity of

specific relevant phosphorylation targets was not known. Our findings fill this gap by revealing that central element proteins (SYCP1, TEX12 and SYCE1), a lateral element protein (SYCP2) and HORMA-domain proteins (HORMAD1 and 2) are among the proteins phosphorylated during the G2/MI transition. Phosphorylation of these SC components is dependent on kinase activity inhibited by BI 2536. Importantly, the amino acid consensus sequence for PLK1, [D/N/E/Y]-X-S/T-[F/φ; no P]-[φ/X] (Alexander et al., 2011) is present in these SC proteins. SYCP1 contains 7 and TEX12 contains 2 PLK1 phosphorylation consensus sites. We showed that SYCP1 and TEX12 are phosphorylated by PLK1, but not by PLK2–4 in vitro. Moreover, a large-scale tissue-specific phosphoproteome study reported that SYCP1 is phosphorylated in testes at five unique residues (Huttlin et al., 2010). SYCP1 contains a PLK1 PBD binding motif and it is known that these motifs can be phosphorylated either by a priming kinase such as CDK1–CYCB1 (nonself-priming) or by PLK1 itself (self-priming) which then act as a binding site for PLK1 and stimulate subsequent phosphorylation of the substrate at PLK1 consensus sites. Both nonself- and self-priming models are implicated for SYCP1 phosphorylation by our work showing that SYCP1 is efficiently phosphorylated by PLK1 alone, but is also phosphorylated by CDK1–CYCB1 in vitro. TEX12 does not contain a PDB binding motif, but it is possible that once PLK1 is bound to a SYCP1 PBD binding motif, it could phosphorylate TEX12 by 'distributive phosphorylation' (Park et al., 2010). Indeed this mechanism of phosphorylation has been recently described for PLK1 mediated phosphorylation of the Augmin subunit HAUS8 (formerly HICE1), which is required for Augmin–microtubule interaction and microtubule-based microtubule nucleation (Johmura et al., 2011). In sum, several lines of evidence presented here suggest PLK1 could act directly on SC substrates to promote desynapsis. However, another, not mutually exclusive, possibility is that PLK1 acts more indirectly, through promotion of other (yet unknown) G2/MI transition events that lead to SC phosphorylation and desynapsis.

Spermatocyte SC protein phosphorylation events were initially detected by assays using ex vivo OA-induced prophase exit. Nonetheless, the modifications are also observed in CIP assays of spermatocytes freshly retrieved from testes and are thus highly likely to be of biological relevance. At 22 dpp, when G2/MI spermatocytes are abundant among the germ cells retrieved from testes, the central elements are phosphorylated. Furthermore, we observed that a central element protein, SYCE1, is present as a single band at the times when early to mid-prophase spermatocytes are abundant (10–16 dpp), but a slower migrating phosphorylated form of SYCE1 was evident when diplotene spermatocytes (those undergoing desynapsis) were abundant (19–22 dpp), suggesting the possibility that SYCE1 is phosphorylated during desynapsis as it is removed from the SC.

Protein interaction studies have been used to determine how the SC central elements interact with one another (Bolcun-Filas et al., 2007; Costa et al., 2005; Hamer et al., 2006; Hamer et al., 2008; Schramm et al., 2011). From these studies, a model for SC assembly emerges whereby SYCP1 molecules forms head to head dimers via their N-termini, an interaction locked in place by multimers of SYCE1. To initiate synapsis, the C-termini of SYCP1 associate with axial (lateral) element proteins that interact with the chromatin of each homolog. SYCE2 and two interacting partners, SYCE3 and TEX12, bind with the

chromatin-associated SYCP1–SYCE1 complexes, polymerizing them to create the SC (Bolcun-Filas et al., 2007; Costa and Cooke, 2007; Schramm et al., 2011). From our work, we can now extend this with a model for SC disassembly, whereby PLK1 phosphorylates central element proteins SYCP1 and TEX12, thereby contributing to (and perhaps initiating) SC central element disassembly, perhaps by disrupting protein–protein interactions. Additionally, PLK1 mediates (directly or indirectly) the phosphorylation of the central element protein SYCE1, lateral element protein SYCP2 and the HORMAD proteins, events that could be required for the disassembly of the SC central elements.

In conclusion, we show that PLK stimulates the disassembly of the SC during the G2/MI transition. Concurrent with SC disassembly, central element components, notably SYCP1 and TEX12 are phosphorylated, and these are substrates of PLK1 in vitro. These findings do not exclude earlier meiotic roles for PLK; ultimately conditional mutation studies will provide a timeline of PLK action in spermatocytes. Our results contribute to experimentally testable models of desynapsis and SC disassembly. Future endeavors should identify specific phosphorylation sites on SC proteins, and SC protein mutants lacking the phosphorylation sites will contribute to resolving their role in desynapsis and meiotic progress.

Materials and Methods

Animals

Mouse germ-cell isolation and culture

Isolation of mixed germ cells from testes was performed using techniques previously described (Bellvé, 1993; La Salle et al., 2009). Pachytene spermatocytes were enriched using a 2–4% BSA gradient generated in a STA-PUT sedimentation chamber (ProScience Inc.) as previously described (Bellvé, 1993; La Salle et al., 2009; Sun and Handel, 2008). Highly enriched pachytene spermatocytes (2.5×10^6 cells/ml) were cultured for 10 hours at 32°C in 5% CO_2 in HEPES (25 mM)-buffered MEMα culture medium (Sigma) supplemented with 25 mM $NaHCO_3$, 5% fetal bovine serum (Atlanta Biologicals), 10 mM sodium lactate, 59 µg/ml penicillin, and 100 µg/ml streptomycin. To initiate the G2/MI transition, cultured pachytene spermatocytes were treated with 5 µM okadaic acid (OA; Calbiochem). To inhibit PLKs, cultured spermatocytes were treated with 100 nM BI 2536 (Selleck Chemicals) diluted in DMSO 0.5 hour prior to OA addition and controls were treated with DMSO alone. For SC disassembly kinetic analyses spermatocytes were harvested and processed as nuclear spreads (see below) at 0, 0.5, 1.0, 1.5, 2.0, 2.5, 3.0, 4.0 and 5.0 hours after OA treatment. For protein analyses spermatocytes were harvested at 0, 2.5 and 5.0 hours after OA treatment for protein extraction as described below.

Transcript expression analysis

mRNA was prepared from enriched germ cells using the QIAGEN RNA purification kit. Following purification RNA was treated with DNase and the RNA purity and concentration was assessed using a ND1000 Nanodrop spectrophotometer. cDNA was synthesized via a reverse transcriptase reaction (QIAGEN). 10 ng of cDNA was used as a template for standard PCR (58°C annealing, 70°C, 30 sec extension for 25 or 35 cycles) and reactions were assessed via standard agarose gel electrophoresis. Primers used are presented in supplementary material Table S1.

Protein analyses

Protein was extracted from germ cells using RIPA buffer (Santa Cruz) or NP40 buffer (150 mM NaCl, 50 mM Tris-HCl, 1% NP40, pH 8.0) containing 1×protease inhibitor cocktail (Roche). Protein concentration was calculated using a BCA protein assay kit (Pierce). For enriched germ cells 20 µl of 1 mg/ml protein extract was loaded per lane on SDS polyacrylamide gels. For STAPUT

purified pachytene cells 20 µl of 0.1 mg/ml was loaded per lane on SDS polyacrylamide gels. Following protein separation via standard SDS-PAGE, proteins were transferred to PVDF membranes using semi-dry western blotting apparatus (Bio-Rad). Primary antibodies and dilution used are presented in supplementary material Table S2. At a 1:20,000 dilution, Invitrogen horseradish peroxidase-conjugated antibodies rabbit anti-mouse (R21455), rabbit anti-guinea pig (NO. 614620), goat anti-rabbit (A10533), rabbit anti-goat (R21459) were used as secondary antibodies. The presence of antibodies on the PVDF membranes was detected by treatment with Pierce ECL western blotting substrate (Thermo Scientific) and exposure to KODAK Blue XB film.

Calf intestinal phosphatase (CIP) assays
Protein from enriched pachytene spermatocytes that had been incubated with OA for 5 hours was extracted into NP40 buffer. Protein extract was used in standard CIP assays (New England Biosciences), and as controls reactions without CIP and reactions containing PhosSTOP (Roche), which inhibits CIP function, were also prepared. CIP reactions were incubated at 37℃ for 60 min, then SDS PAGE loading buffer was added followed by heat mediated protein denaturation and samples were assessed using SDS-PAGE and western blotting.

In vitro kinase assays
SYCP1–Myc/DDK and the corresponding empty vector cell lysate control (Origene); TEX12–GST (ProteinTech Group), SYCE1–GST (ProteinTech Group) and the GST protein control (Abcam); TEX12–6*His, SYCE1–6*His and the empty vector cell lysate control (ProteinTech Group) were used as substrates for *in vitro* kinase assays. The substrates (2.5 µg) were combined with Mg/ATP cocktail (7.5 mM MgCl, 500 µM ATP, 2 mM MOPS, pH 7.2, 2.5 mM β-glycerol, 0.5 mM EGTA, 0.1 mM sodium orthovanadate, 0.1 mM DTT), 2% DMSO or 25 nM of BI 2536 in DMSO, 1.5 µCi [γ-^{32}P]ATP; the kinases used were recombinant PLK1 (Carna Bioscience and Abcam), PLK2, PLK3, PLK4 and CDK1/CYB1 (Carna Bioscience). Reactions were carried out at 32℃ for 20 min, SDS PAGE loading buffer was added followed by heat-mediated protein denaturation and samples were assessed using SDS-PAGE, western blotting and autoradiography. Substrates and kinases used in these assays correspond to the human sequences.

Spread chromatin analysis
Germ cell nuclear spreads were prepared as previously described (Cobb et al., 1999; Cobb et al., 1997; Sun and Handel, 2008). Primary antibodies and dilution used are presented in supplementary material Table S2. Secondary antibodies against rabbit, rat, mouse and guinea pig IgG and conjugated to Alexa Fluor 488, 594 or 647 (Molecular Probes) were used at 1:500 dilution. Nuclear spreads were mounted in Vectashield + DAPI medium (Vector Laboratories). For antibody pre-absorption, the PLK antibodies were pre-incubated with the corresponding PLK proteins (Carna Bioscience) for 45 min at 32℃. Nuclear spread images were captured using a Zeiss Axio Observer Z1 linked to an AxioCam MR Rev3 camera and analyzed with the AxioVision V4.8 image software.

Supplementary material available online at
http://jcs.biologists.org/lookup/suppl/doi:10.1242/jcs.105015/-/DC1

References
Abe, S., Nagasaka, K., Hirayama, Y., Kozuka-Hata, H., Oyama, M., Aoyagi, Y., Obuse, C. and Hirota, T. (2011). The initial phase of chromosome condensation requires Cdk1-mediated phosphorylation of the CAP-D3 subunit of condensin II. *Genes Dev.* 25, 863-874.

Alexander, J., Lim, D., Joughin, B. A., Hegemann, B., Hutchins, J. R. A., Ehrenberger, T., Ivins, F., Sessa, F., Hudecz, O., Nigg, E. A. et al. (2011). Spatial exclusivity combined with positive and negative selection of phosphorylation motifs is the basis for context-dependent mitotic signaling. *Sci. Signal.* 4, ra42.

Bellvé, A. R. (1993). Purification, culture, and fractionation of spermatogenic cells. *Methods Enzymol.* 225, 84-113.

Bellvé, A. R., Millette, C. F., Bhatnagar, Y. M. and O'Brien, D. A. (1977). Dissociation of the mouse testis and characterization of isolated spermatogenic cells. *J. Histochem. Cytochem.* 25, 480-494.

Bolcun-Filas, E., Costa, Y., Speed, R., Taggart, M., Benavente, R., De Rooij, D. G. and Cooke, H. J. (2007). SYCE2 is required for synaptonemal complex assembly, double strand break repair, and homologous recombination. *J. Cell Biol.* 176, 741-747.

Clyne, R. K., Katis, V. L., Jessop, L., Benjamin, K. R., Herskowitz, I., Lichten, M. and Nasmyth, K. (2003). Polo-like kinase Cdc5 promotes chiasmata formation and cosegregation of sister centromeres at meiosis I. *Nat. Cell Biol.* 5, 480-485.

Cobb, J., Reddy, R. K., Park, C. and Handel, M. A. (1997). Analysis of expression and function of topoisomerase I and II during meiosis in male mice. *Mol. Reprod. Dev.* 46, 489-498.

Cobb, J., Cargile, B. and Handel, M. A. (1999). Acquisition of competence to condense metaphase I chromosomes during spermatogenesis. *Dev. Biol.* 205, 49-64.

Cohen, P. E., Pollack, S. E. and Pollard, J. W. (2006). Genetic analysis of chromosome pairing, recombination, and cell cycle control during first meiotic prophase in mammals. *Endocr. Rev.* 27, 398-426.

Costa, Y. and Cooke, H. J. (2007). Dissecting the mammalian synaptonemal complex using targeted mutations. *Chromosome Res.* 15, 579-589.

Costa, Y., Speed, R., Ollinger, R., Alsheimer, M., Semple, C. A., Gautier, P., Maratou, K., Novak, I., Höög, C., Benavente, R. et al. (2005). Two novel proteins recruited to synaptonemal complex protein 1 (SYCP1) are at the centre of meiosis. *J. Cell Sci.* 118, 2755-2762.

de Cárcer, G., Manning, G. and Malumbres, M. (2011). From Plk1 to Plk5: functional evolution of polo-like kinases. *Cell Cycle* 10, 2255-2262.

Dix, D. J., Allen, J. W., Collins, B. W., Poorman-Allen, P., Mori, C., Blizard, D. R., Brown, P. R., Goulding, E. H., Strong, B. D. and Eddy, E. M. (1997). HSP70-2 is required for desynapsis of synaptonemal complexes during meiotic prophase in juvenile and adult mouse spermatocytes. *Development* 124, 4595-4603.

Dobson, M. J., Pearlman, R. E., Karaiskakis, A., Spyropoulos, B. and Moens, P. B. (1994). Synaptonemal complex proteins: occurrence, epitope mapping and chromosome disjunction. *J. Cell Sci.* 107, 2749-2760.

Edelmann, W., Cohen, P. E., Kane, M., Lau, K., Morrow, B., Bennett, S., Umar, A., Kunkel, T., Cattoretti, G., Chaganti, R. et al. (1996). Meiotic pachytene arrest in MLH1-deficient mice. *Cell* 85, 1125-1134.

Elia, A. E. H., Rellos, P., Haire, L. F., Chao, J. W., Ivins, F. J., Hoepker, K., Mohammad, D., Cantley, L. C., Smerdon, S. J. and Yaffe, M. B. (2003). The molecular basis for phosphodependent substrate targeting and regulation of Plks by the Polo-box domain. *Cell* 115, 83-95.

Fernandez-Capetillo, O., Mahadevaiah, S. K., Celeste, A., Romanienko, P. J., Camerini-Otero, R. D., Bonner, W. M., Manova, K., Burgoyne, P. and Nussenzweig, A. (2003). H2AX is required for chromatin remodeling and inactivation of sex chromosomes in male mouse meiosis. *Dev. Cell* 4, 497-508.

Hamer, G., Gell, K., Kouznetsova, A., Novak, I., Benavente, R. and Höög, C. (2006). Characterization of a novel meiosis-specific protein within the central element of the synaptonemal complex. *J. Cell Sci.* 119, 4025-4032.

Hamer, G., Wang, H., Bolcun-Filas, E., Cooke, H. J., Benavente, R. and Höög, C. (2008). Progression of meiotic recombination requires structural maturation of the central element of the synaptonemal complex. *J. Cell Sci.* 121, 2445-2451.

Handel, M. A. (2004). The XY body: a specialized meiotic chromatin domain. *Exp. Cell Res.* 296, 57-63.

Handel, M. A. and Schimenti, J. C. (2010). Genetics of mammalian meiosis: regulation, dynamics and impact on fertility. *Nat. Rev. Genet.* 11, 124-136.

Handel, M. A., Caldwell, K. A. and Wiltshire, T. (1995). Culture of pachytene spermatocytes for analysis of meiosis. *Dev. Genet.* 16, 128-139.

Harper, N. C., Rillo, R., Jover-Gil, S., Assaf, Z. J., Bhalla, N. and Dernburg, A. F. (2011). Pairing centers recruit a Polo-like kinase to orchestrate meiotic chromosome dynamics in *C. elegans*. *Dev. Cell* 21, 934-947.

Harris, R. M., Weiss, J. and Jameson, J. L. (2011). Male hypogonadism and germ cell loss caused by a mutation in Polo-like kinase 4. *Endocrinology* 152, 3975-3985.

Holloway, J. K., Booth, J., Edelmann, W., McGowan, C. H. and Cohen, P. E. (2008). MUS81 generates a subset of MLH1-MLH3-independent crossovers in mammalian meiosis. *PLoS Genet.* 4, e1000186.

Huttlin, E. L., Jedrychowski, M. P., Elias, J. E., Goswami, T., Rad, R., Beausoleil, S. A., Villén, J., Haas, W., Sowa, M. E. and Gygi, S. P. (2010). A tissue-specific atlas of mouse protein phosphorylation and expression. *Cell* 143, 1174-1189.

Johmura, Y., Soung, N.-K., Park, J.-E., Yu, L.-R., Zhou, M., Bang, J. K., Kim, B.-Y., Veenstra, T. D., Erikson, R. L. and Lee, K. S. (2011). Regulation of microtubule-based microtubule nucleation by mammalian polo-like kinase 1. *Proc. Natl. Acad. Sci. USA* 108, 11446-11451.

Jordan, P., Copsey, A., Newnham, L., Kolar, E., Lichten, M. and Hoffmann, E. (2009). Ipl1/Aurora B kinase coordinates synaptonemal complex disassembly with cell cycle progression and crossover formation in budding yeast meiosis. *Genes Dev.* 23, 2237-2251.

Kang, Y. H., Park, J.-E., Yu, L.-R., Soung, N.-K., Yun, S.-M., Bang, J. K., Seong, Y.-S., Yu, H., Garfield, S., Veenstra, T. D. et al. (2006). Self-regulated Plk1 recruitment to kinetochores by the Plk1-PBIP1 interaction is critical for proper chromosome segregation. *Mol. Cell* **24**, 409-422.

Kishimoto, T. (2003). Cell-cycle control during meiotic maturation. *Curr. Opin. Cell Biol.* **15**, 654-663.

La Salle, S., Sun, F. and Handel, M. A. (2009). Isolation and short-term culture of mouse spermatocytes for analysis of meiosis. *Meiosis Vol. 2* (ed. S. Keeney) *Methods in Molecular Biology* Vol. 558, pp. 279-297. Cincinnati, OH: Humana Press.

Labella, S., Woglar, A., Jantsch, V. and Zetka, M. (2011). Polo kinases establish links between meiotic chromosomes and cytoskeletal forces essential for homolog pairing. *Dev. Cell* **21**, 948-958.

Lipkin, S. M., Moens, P. B., Wang, V., Lenzi, M., Shanmugarajah, D., Gilgeous, A., Thomas, J., Cheng, J., Touchman, J. W., Green, E. D. et al. (2002). Meiotic arrest and aneuploidy in MLH3-deficient mice. *Nat. Genet.* **31**, 385-390.

Ma, S., Charron, J. and Erikson, R. L. (2003). Role of Plk2 (*Snk*) in mouse development and cell proliferation. *Mol. Cell. Biol.* **23**, 6936-6943.

Matos, J., Blanco, M. G., Maslen, S., Skehel, J. M. and West, S. C. (2011). Regulatory control of the resolution of DNA recombination intermediates during meiosis and mitosis. *Cell* **147**, 158-172.

Moens, P. B., Kolas, N. K., Tarsounas, M., Marcon, E., Cohen, P. E. and Spyropoulos, B. (2002). The time course and chromosomal localization of recombination-related proteins at meiosis in the mouse are compatible with models that can resolve the early DNA-DNA interactions without reciprocal recombination. *J. Cell Sci.* **115**, 1611-1622.

Myer, D. L., Robbins, S. B., Yin, M., Boivin, G. P., Liu, Y., Greis, K. D., Bahassi, M. and Stambrook, P. J. (2011). Absence of polo-like kinase 3 in mice stabilizes Cdc25A after DNA damage but is not sufficient to produce tumors. *Mutat. Res.* **714**, 1-10.

Park, J.-E., Soung, N.-K., Johmura, Y., Kang, Y. H., Liao, C., Lee, K. H., Park, C. H., Nicklaus, M. C. and Lee, K. S. (2010). Polo-box domain: a versatile mediator of polo-like kinase function. *Cell. Mol. Life Sci.* **67**, 1957-1970.

Petronczki, M., Lénárt, P. and Peters, J.-M. (2008). Polo on the rise – from mitotic entry to cytokinesis with Plk1. *Dev. Cell* **14**, 646-659.

Royo, H., Polikiewicz, G., Mahadevaiah, S. K., Prosser, H., Mitchell, M., Bradley, A., de Rooij, D. G., Burgoyne, P. S. and Turner, J. M. A. (2010). Evidence that meiotic sex chromosome inactivation is essential for male fertility. *Curr. Biol.* **20**, 2117-2123.

Santamaria, A., Wang, B., Elowe, S., Malik, R., Zhang, F., Bauer, M., Schmidt, A., Sillje, H. H. W., Koerner, R. and Nigg, E. A. (2010). The Plk1-dependent phosphoproteome of the early mitotic spindle. *Mol. Cell. Proteomics* **10**, M110.004457.

Schramm, S., Fraune, J., Naumann, R., Hernandez-Hernandez, A., Höög, C., Cooke, H. J., Alsheimer, M. and Benavente, R. (2011). A novel mouse synaptonemal complex protein is essential for loading of central element proteins, recombination, and fertility. *PLoS Genet.* **7**, e1002088.

Shen, W., Ahmad, F., Hockman, S., Ma, J., Omi, H., Raghavachari, N. and Manganiello, V. (2010). Female infertility in PDE3A(-/-) mice: polo-like kinase 1 (Plk1) may be a target of protein kinase A (PKA) and involved in meiotic arrest of oocytes from PDE3A(-/-) mice. *Cell Cycle* **9**, 4720-4734.

Sourirajan, A. and Lichten, M. (2008). Polo-like kinase Cdc5 drives exit from pachytene during budding yeast meiosis. *Genes Dev.* **22**, 2627-2632.

Steegmaier, M., Hoffmann, M., Baum, A., Lénárt, P., Petronczki, M., Krssák, M., Gürtler, U., Garin-Chesa, P., Lieb, S., Quant, J. et al. (2007). BI 2536, a potent and selective inhibitor of polo-like kinase 1, inhibits tumor growth in vivo. *Curr. Biol.* **17**, 316-322.

Strebhardt, K. (2010). Multifaceted polo-like kinases: drug targets and antitargets for cancer therapy. *Nat. Rev. Drug Discov.* **9**, 643-660.

Sun, F. and Handel, M. A. (2008). Regulation of the meiotic prophase I to metaphase I transition in mouse spermatocytes. *Chromosoma* **117**, 471-485.

Sun, F., Palmer, K. and Handel, M. A. (2010). Mutation of *Eif4g3*, encoding a eukaryotic translation initiation factor, causes male infertility and meiotic arrest of mouse spermatocytes. *Development* **137**, 1699-1707.

Tarsounas, M., Pearlman, R. E. and Moens, P. B. (1999). Meiotic activation of rat pachytene spermatocytes with okadaic acid: the behaviour of synaptonemal complex components SYN1/SCP1 and COR1/SCP3. *J. Cell Sci.* **112**, 423-434.

Turner, J. M. A. (2007). Meiotic sex chromosome inactivation. *Development* **134**, 1823-1831.

Wiltshire, T., Park, C., Caldwell, K. A. and Handel, M. A. (1995). Induced premature G2/M-phase transition in pachytene spermatocytes includes events unique to meiosis. *Dev. Biol.* **169**, 557-567.

Wojtasz, L., Daniel, K., Roig, I., Bolcun-Filas, E., Xu, H., Boonsanay, V., Eckmann, C. R., Cooke, H. J., Jasin, M., Keeney, S. et al. (2009). Mouse HORMAD1 and HORMAD2, two conserved meiotic chromosomal proteins, are depleted from synapsed chromosome axes with the help of TRIP13 AAA-ATPase. *PLoS Genet.* **5**, e1000702.

Xiang, Y., Takeo, S., Florens, L., Hughes, S. E., Huo, L.-J., Gilliland, W. D., Swanson, S. K., Teeter, K., Schwartz, J. W., Washburn, M. P. et al. (2007). The inhibition of polo kinase by matrimony maintains G2 arrest in the meiotic cell cycle. *PLoS Biol.* **5**, e323.

Yanowitz, J. (2010). Meiosis: making a break for it. *Curr. Opin. Cell Biol.* **22**, 744-751.

Zhu, D., Dix, D. J. and Eddy, E. M. (1997). HSP70-2 is required for CDC2 kinase activity in meiosis I of mouse spermatocytes. *Development* **124**, 3007-3014.